International Journal of Soft Computing 5 (6): 219-222, 2010
ISSN: 1816-9503
© Medwell Journals, 2010

Comparison of Monte Carlo and Hydrodynamic Model in Electron Transport Characteristics of n^+-i (n)-n^+ ZnO Diode

H. Arabshahi and M. Rezaee Rokn-Abadi
Department of Physics, Ferdowsi University of Mashhad, Mashhad, Iran

Abstract: An ensemble Monte Carlo simulation has been used to model electron transport in n^+-i (n)-n^+ ZnO diode at 300 K in comparison with hydrodynamic approach. Electronic states within the conduction band are represented by non-parabolic ellipsoidal valleys centered on important symmetry points of the Brillouin zone. An original decomposition of velocity and energy profiles along the structure in terms of field, convective and diffusion contributions are presented. The anode voltage ranges from 0-3.75 V. The distributions of electron energies and electron velocities and the profiles of the electron density, electric field and average electron velocity are computed. Based on these data, the excellent agreement of the hydrodynamic approach with Monte Carlo simulations is discussed.

Key words: Ensemble Monte Carlo, hydrodynamic, anode voltage, diffusion contributions, Iran

INTRODUCTION

Wide-bandgap semiconductors such as 6H-SiC (3.0 eV, at 2 K) and GaN (3.5 eV) have come to the forefront in the past decade because of an increasing need for short-wavelength photonic devices and high-power, high-frequency electronic devices and because of breakthroughs in high-quality growths of these materials.

On the other hand, another wide-band gap semiconductor, ZnO (3.4 eV) has not received the same attention, probably because this material has been perceived as being useful only in its polycrystalline form. Indeed, polycrystalline ZnO has found numerous applications in such diverse areas as facial powders, piezoelectric transducers, varistors, phosphors and transparent conducting films. Recently however, large area bulk growth has been achieved (Tsukazaki *et al*., 2005) and furthermore, several epitaxial methods have produced excellent material (Makino *et al*., 2001, 2002; Bellotti *et al*., 1999; Look *et al*., 1998; Chen *et al*., 1998; Moglestue, 1993; Jacoboni and Lugli, 1989; Ridley, 1997; Chattopadhya and Queisser, 1981). Also, quantum wells have been successfully grown by alloying with Mg or Cd (Di and Brennan, 1991). Thus, ZnO is now being proposed for the same applications as those listed above for GaN and SiC. In fact, ZnO has several fundamental advantages over its chief competitor, GaN: its free exciton is bound with 60 meV much higher than that of GaN (21-25 meV), it has a native substrate, wet chemical processing is possible and it is more resistant to radiation damage (although, both are much better than Si or GaAs). In recent years, various theoretical approaches have been developed and used to calculate electronic transport characteristics in semiconductor devices. Among these methods the hydrodynamic approach which combines the simplicity of the drift-diffusion model with the possibility of accounting for non-local effects such as velocity overshoot has emerged as a very reliable technique (Mansour *et al*., 1991). In general, the hydrodynamic description is based on velocity and energy conservation equations which are derived from the Boltzmann kinetic equation.

However, such a derivation implies the introduction of several assumptions to close the system of conservation equations and as a consequence there exists a certain degree of freedom in the choice of the parameters to be used. The aim of this study is to apply the hydrodynamic model to the case of submicron n^+-i (n)-n^+ ZnO structures. The comparison between the hydrodynamic model and a Monte Carlo simulation is taken as a validating proof of the hydrodynamic model. In particular, an original decomposition procedure involving the velocity and energy profiles in terms of field, convective and diffusive components has enabled us to carry out a detailed interpretation of electron transport in submicron n^+-i (n)-n^+ diode.

MATERIALS AND METHODS

For a one-dimensional geometry, the hydrodynamic approach model equations consist of the continuity Eq. 1:

$$\frac{\partial n}{\partial t} + \nabla . j = 0 \qquad (1)$$

Corresponding Author: H. Arabshahi, Department of Physics, Ferdowsi University of Mashhad, Mashhad, Iran

For negligible charge carrier generation and recombination, the momentum balance equation given by:

$$\frac{\partial p}{\partial t} + (\nabla p)v + (p\nabla)v = -enE - \nabla(nkT) - \frac{p}{\tau_p} \quad (2)$$

Or alternatively (only for x-component):

$$\frac{[m^*(\varepsilon')nv_x]}{\partial t} + \nabla[m^*(\varepsilon')nv_x v] = -qnE_x - \frac{\partial(nkT)}{\partial x} - \frac{m^*(\varepsilon')nv_x}{\tau_p(t')} \quad (3)$$

And the energy balance Eq. 4 is:

$$\frac{\partial \varepsilon}{\partial t} + \nabla(v\varepsilon) = -qnvE - \nabla(nkTv) - \nabla(-k\nabla T) - \frac{\varepsilon - 3/2nkT_l}{\tau_\varepsilon(\varepsilon')} \quad (4)$$

where, n, ε ($\varepsilon' = \varepsilon/n$) and v are the electron density, the electron energy density (average electron energy) and the electron drift velocity, respectively. v_x is the x-component of the electron drift velocity and $p = m^*nv$ is the momentum density.

Corresponding equations are valid for the y and z components. T is the electron temperature and $\varepsilon'_0 = 3/2kT_l$ is the average termal equilibrium energy of electrons where T_l is the lattice temperature. The electronic current density j inside the active device is j = -nev so the total current density is:

$$j_t = -nev + \varepsilon_0\varepsilon_r \frac{\partial E}{\partial t} \quad (5)$$

The momentum relaxation time $\tau_p(\varepsilon')$ is related to the mobility of the electrons via $\mu(\varepsilon') = e/m^*(\varepsilon')\,\tau_p(\varepsilon')$ and the energy relaxation time $\tau_p(\varepsilon')$ describes the exchange of energy between the heated electron gas and the lattice. τ_p and τ_ϵ and the effective electron mass m* are assumed to be functions of the mean electron energy. The hydrodynamic equations, together with Poisson's Eq. 6:

$$\Delta\phi = \nabla E = -\frac{e}{\varepsilon_0\varepsilon_r}(N_d^+ - n) \quad (6)$$

Form a complete set of equations that can be used to solve for the electron density, velocity, energy and electric field for given boundary conditions. The hydrodynamic model based on Eq. 1-4 has an evident advantage in that it gives the possibility of verifying directly the assumptions used to close the system of conservation equations. Indeed, the spatial profiles of both velocity and energy can be directly calculated with the Monte Carlo simulation for the structure investigated and compared with those which can be deduced from the hydrodynamic calculations. Self-consistent Monte Carlo simulation was performed using an analytical band structure model consisting of three non-parabolic ellipsoidal valleys (Arabshahi *et al*., 2007; Arabshahi, 2007a).

The scattering mechanisms considered in the model are acoustic, polar optical, ionized impurity, piezoelectric and nonequivalent intervalley scattering. The nonequivalent intervalley scattering is between the Γ, U and K. Acoustic and piezoelectric scattering are assumed elastic and the absorption and emission rates are combined under the equipartition approximation which is valid for lattice temperatures above 77 K.

Elastic ionized impurity scattering is described using the screened Coulomb potential of the Brooks-Herring model. Steady-state results of high field transport studies have been obtained for lattice temperatures up to 300 K, in order to gain some insight into the hot carrier transport and the energy distribution function that would be generated in the gate-drain region of a power field effect transistor.

The overall diode length which is used in both hydrodynamic and Monte Carlo model has 0.6 μm in the x-direction. A lightly doped active layer (n-layer) is sandwiched between cathode and anode layers which are abruptly doped with a donor density of 10^{24} m^{-3} (Shimada *et al*., 1998; Joshi, 1994; Arabshahi, 2007b). The length of the active layer is 0.2 μm. Approximately 10^4 particles are used in the simulation and calculations are performed at room temperature.

The applied anode voltage V_a is varied between 0 and 3.75 V to investigate the effects of field variations on the transport properties. This range of voltages is large enough that velocity overshoot and intervalley transfer effects occur.

RESULTS AND DISCUSSION

The electron density and electric field profiles calculated with the hydrodynamic and Monte Carlo models are shown in Fig. 1a and b, respectively. An excellent agreement between the results of the 2 approaches is found.

By comparing the value of the electron density through the device, researchers conclude that the electrons diffuse from the cathode and anode into the active layer and are accelerated towards the anode by the

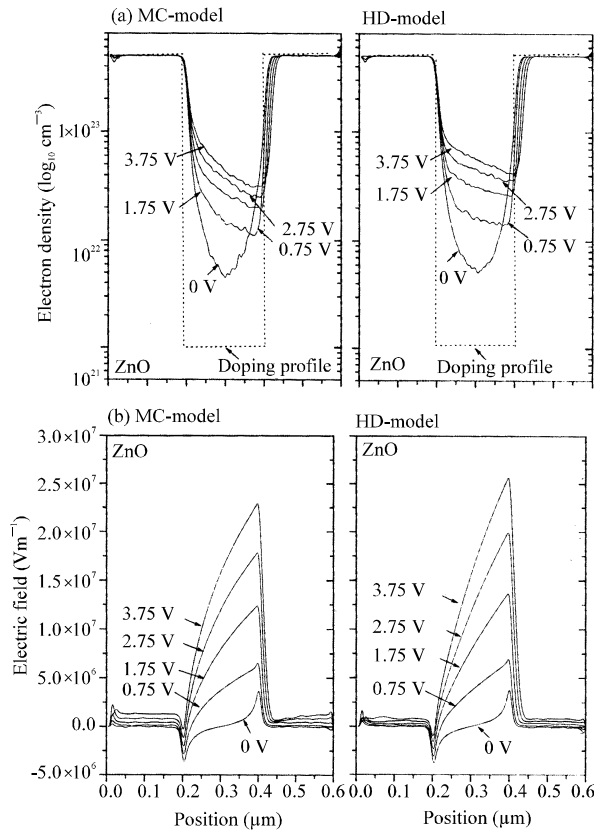

Fig. 1: Spatial profiles of electron density and electric field calculated with Monte Carlo and hydrodaynamic approaches for the 0.6 μm ZnO n^+-i (n)-n^+ diode with doping levels n = 10^{21} m^{-3} and n^+ = 10^{24} m^{-3}. The applied anode voltage is varied between 0-3.75 V and the results are at room temperature

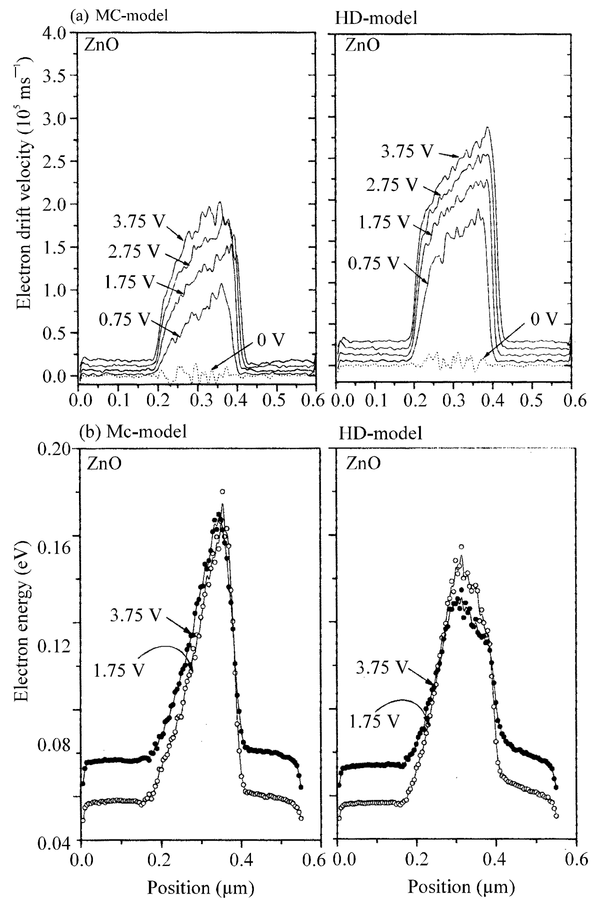

Fig. 2: Spatial profiles of (a) drift velocity and (b) electron average energy calculated with Monte Carlo and hydrodaynamic approaches for the 0.6 μm ZnO n^+-i (n)-n^+ diode with doping levels n = 10^{21} m^{-3} and n^+ = 10^{24} m^{-3}. The applied anode voltage is varied between 0-3.75 V and the results are at room temperature

field. The resulting space charge causes the departure from a uniform electric field clearly shown in Fig. 1b. It is apparent from Fig. 1b that both hydrodynamic and Monte Carlo models show that essentially all the potential is dropped in the active layer. However, as a result of the inhomogeneous space charge the field does vary substantially with position, resulting a maximum magnitude near the anode.

As the next step, Fig. 2a and b shows the comparison between the hydrodynamic and Monte Carlo calculations for the velocity and energy profiles.

Even in this case a good agreement between the 2 approaches is achieved. Figure 2a shows that the average drift velocity in the active layer has a maximum value of about 2×10^5 m sec^{-1} at 300 K. The plot of average electron kinetic energy across the device (Fig. 2b) provides further information on the dynamics. The electrons reach an average energy between 0.14 and 0.16 eV near the anode region and the more energetic electrons in the distribution have sufficient energy to transfer to the upper valleys.

Figure 3a and b shows the distribution of energy and velocity parallel to the electric field throughout the 0.6 μm ZnO n^+-i (n)-n^+ diode in the steady-state at 300 K with a bias of 3.75 V when the active layer doping level is 10^{24} m^{-3}.

It is apparent that there is a significant concentration in the satellite valleys on the anode side of the active layer. These electrons have attained enough energy under the action of the electric field to be scattered into satellite valleys.

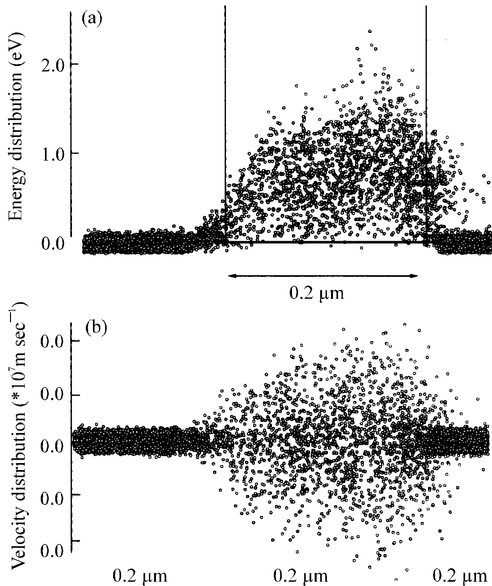

Fig. 3: (a) Energy distribution and (b) velocity distribution throughout the simulated 0.6 μm ZnO n^+-i (n)-n^+ diode. The applied anode voltage is V_a = 3.75 V and the results are at room temperature

CONCLUSION

An ensemble Monte Carlo simulation has been carried out to simulate the electron transport in n^+-i (n)-n^+ ZnO diode at 300 K in comparison with hydrodynamic approach. The hydrodynamic model has been validated by comparison with a Monte Carlo particle simulator. An original decomposition of electron velocity and energy profiles in terms of field, convective and diffusive contributions has evidenced their importance and their mutual balancing near the homo-junctions. The electrons injected from the cathode initially travel quasi-ballistically but there is substantial transfer to the upper satellite valleys as the anode is approached, resulting in a reduced average electron velocity in that region. The peak drift velocity ranges from 1×10^5-2.5×10^5 m sec^{-1} with a donor density of 10^{21} m^{-3} and an active layer length of 0.2 μm.

ACKNOWLEDGEMENT

This research is supported by the Ferdowsi University of Mashhad through a contract with Vice President for Research and Technology.

REFERENCES

Arabshahi, H., 2007a. Comparison of high field electron transport properties in wurtzite and zincblende phase GaN at room temperature. Mod. Phys. Lett. B, 21: 199-206.

Arabshahi, H., 2007b. MONTE CARLO simulations of steady-state transport in wurtzite phase GaN submicrometer n+nn+ diode. Mod. Phys. Lett. B, 21: 287-294.

Arabshahi, H., M.R. Benam and B. Salahi and M. Gholizadeh, 2007. Comparison of high field steady state and transient electron transport in wurtzite GaN, Aln and InN. Mod. Phys. Lett. B, 21: 1715-1721.

Bellotti, E., B.K. Doshi and K.F. Brennan, 1999. Ensemble Monte Carlo study of electron transport in wurtzite InN. J. Applied Phys., 85: 916-923.

Chattopadhya, D. and H.J. Queisser, 1981. Electron scattering by ionized impurities in semiconductors. Rev. Mod. Phys., 53: 745-768.

Chen, Y., D.M. Bagnall, H.J. Koh, K.T. Park, Z.Q. Zhu and T. Yao, 1998. Plasma assisted molecular beam epitaxy of ZnO on c-plane sapphire: Growth and characterization. J. Applied Phys., 84: 3912-3912.

Di, K. and K. Brennan, 1991. Comparison of electron transport properties in ZnS and ZnSe. J. Applied Phys., 69: 3097-3097.

Jacoboni, C. and P. Lugli, 1989. The Monte Carlo Method for Semiconductor and Device Simulation. Springer-Verlag, New York.

Joshi, R.P., 1994. Temperature-dependent electron mobility in GaN: Effects of space charge and interface roughness scattering. Applied Phys. Lett., 65: 223-223.

Look, D.C., D.C. Reynolds, J.R. Sizelove and W.C. Harsch, 1998. Electrical properties of bulk ZnO. Solid State Commun., 105: 399-401.

Makino, T., K. Tamura, C.H. Chia, Y. Segawa, M. Kawasaki, A. Ohtomo and H. Koinuma, 2002. Optical properties of ZnO:Al epilayers: Observation of room-temperature many-body absorption-edge singularity. Phys. Rev. B, 65: 121201-121205.

Makino, T., Y. Segawa and A. Ohtomo, 2001. Band gap engineering based on Mg ZnO and Cd ZnO ternary alloy films. Applied Phys. Lett., 78: 1237-1237.

Mansour, N., K. Di and K. Brennan, 1991. Full band Monte Carlo simulation in GaN material. J. Applied Phys., 70: 6854-6854.

Moglestue, C., 1993. Monte Carlo Simulation of Semiconductor Devices. Chapman and Hall, Netherlands.

Ridley, B.K., 1997. Electrons and Phonons in Semiconductor Multilayers. Cambridge University Press, New York, pp: 352.

Shimada, K., T. Sota and K. Suzuki, 1998. First-principles study on electronic and elastic properties of BN, AlN and GaN. J. Applied Phys., 84: 4951-4958.

Tsukazaki, A., A. Ohtomo, T. Onuma, M. Ohtani and M. Kawasaki *et al*., 2005. Repeated temperature modulation epitaxy for p-type doping and light-emitting diode based on ZnO. Nat. Mater., 4: 42-46.